Eur Radiol (2015) 25:872–882
DOI 10.1007/s00330-014-3457-6

MUSCULOSKELETAL

# Exact monitoring of aortic diameters in Marfan patients without gadolinium contrast: intraindividual comparison of 2D SSFP imaging with 3D CE-MRA and echocardiography

**Simon Veldhoen · Cyrus Behzadi · Thorsten Derlin · Meike Rybczinsky · Yskert von Kodolitsch · Sara Sheikhzadeh · Frank Oliver Henes · Thorsten Alexander Bley · Gerhard Adam · Peter Bannas**

Received: 11 March 2014 / Revised: 28 August 2014 / Accepted: 29 September 2014 / Published online: 15 October 2014


**Abstract**
*Purpose* To assess whether ECG-gated non-contrast 2D steady-state free precession (SSFP) imaging allows for exact monitoring of aortic diameters in Marfan syndrome (MFS) patients using non-ECG-gated contrast-enhanced 3D magnetic resonance angiography (CE-MRA) and echocardiography for intraindividual comparison.
*Methods* Non-ECG-gated CE-MRA and ECG-gated non-contrast SSFP at 1.5 T were prospectively performed in 50 patients. Two readers measured aortic diameters on para-sagittal images identically aligned with the aortic arch at the sinuses of Valsalva, sinotubular junction, ascending/descending aorta and aortic arch. Image quality was assessed on a three-point scale. Aortic root diameters acquired by echocardiography were used as reference.
*Results* Intra- and interobserver variances were smaller for SSFP at the sinuses of Valsalva ($p$=0.002; $p$=0.002) and sinotubular junction ($p$=0.014; $p$=0.043). Image quality was better in SSFP than in CE-MRA at the sinuses of Valsalva ($p$<0.0001), sinotubular junction ($p$<0.0001) and ascending aorta ($p$=0.02). CE-MRA yielded higher diameters than SSFP at the sinuses of Valsalva (mean bias, 2.5 mm; $p$<0.0001), and comparison with echocardiography confirmed a higher bias for CE-MRA (7.2±3.4 mm vs. SSFP, 4.7±2.6 mm).
*Conclusion* ECG-gated non-contrast 2D SSFP imaging provides superior image quality with higher validity compared to non-ECG-gated contrast-enhanced 3D imaging. Since CE-MRA requires contrast agents with potential adverse effects, non-contrast SSFP imaging is an appropriate alternative for exact and riskless aortic monitoring of MFS patients.
*Key Points*
- *ECG-gated 2D SSFP imaging provides better image quality than non-ECG-gated contrast-enhanced 3D MRA*
- *ECG-gated 2D SSFP imaging provides higher reproducibility than non-ECG-gated contrast-enhanced 3D MRA*
- *2D SSFP imaging provides higher validity than 3D MRA using echocardiography as reference*
- *ECG-gated non-contrast 2D SFFP imaging allows for riskless monitoring of Marfan patients*

**Keywords** Marfan syndrome · Magnetic resonance angiography · Contrast agents · Sinus Valsalva · Aortic aneurysm

## Introduction

Marfan syndrome (MFS) is a genetic disorder of the connective tissue caused by mutations in the *FBN1* gene encoding the protein fibrilin-1. It shows an autosomal-dominant inheritance and its prevalence has been reported with one in 5,000–10,000 individuals [1]. The syndrome can evoke a wide spectrum of symptoms of varying severity affecting the ocular and skeletal as well as the cardiovascular system [1]. Dilatation of the aortic root is the most common cardiovascular manifestation. The high risk of aortic dissection and consecutive pericardial

S. Veldhoen · T. Bley
Department of Diagnostic and Interventional Radiology, University Medical Center Würzburg, Bavaria, Germany

S. Veldhoen · C. Behzadi · T. Derlin · F. Henes · G. Adam · P. Bannas (✉)
Department of Diagnostic and Interventional Radiology, University Medical Center Hamburg-Eppendorf, Martinistr. 52, 20246 Hamburg, Germany
e-mail: p.bannas@uke.de

M. Rybczinsky · Y. von Kodolitsch · S. Sheikhzadeh
Department of General and Interventional Cardiology, University Medical Center Hamburg-Eppendorf, Hamburg, Germany

tamponade or rupture represent life-threatening complications [2]. Pharmacotherapy reducing the progression rate of aortic dilation and cardiac surgery preventing from aortic dissection could increase the life expectancy by 25 %, but their efficiency still depends on a precise diagnosis at an early stage of the disease [3].

Annual imaging is recommended for monitoring aortic root dimensions [4]. For MFS patients, current guidelines recommend prophylactic aortic root replacement at a threshold diameter of 5.0 cm. In case of high risk for rupture e.g. due to a growing rate of at least 0.5 cm per year, elective surgery is recommended at an external diameter of less than 5.0 cm [5, 6]. As 15 % of MFS patients present with aortic dissection at diameters of 5.0 cm or less, expert centres with vast expertise and good surgical outcome perform surgery at a threshold of 4.5 cm [7, 8]. Hence, imaging modalities that allow precise, reproducible, operator-independent and standardized assessment of the aorta are key in the follow-up of MFS.

Echocardiography, multidetector computed tomography (MDCT) and magnetic resonance imaging (MRI) are available for non-invasive imaging of the aortic root [9]. Especially in adults, echocardiography cannot assess the entire aorta [10] and is highly operator-dependent. MDCT uses radiation and necessitates the application of iodinated contrast. Magnetic resonance angiography (MRA) does not require radiation or iodinated contrast. Excellent image quality covering the entire aorta can be acquired in an observer-independent fashion. Therefore, contrast-enhanced MRA is recommended for imaging of the entire thoracic aorta in patients with congenital heart disease [11].

Several unenhanced MRA techniques, including fast spin-echo and gradient-echo sequences, have been evaluated for imaging of the aorta. Of these, balanced steady-state with free precession (SSFP) techniques are desirable because of their inherent high contrast between blood and background tissues, thereby providing superior imaging of the aortic wall than contrast-enhanced MRA techniques [12, 13]. Recent studies compared non-contrast MRA to standard contrast-enhanced MRA with the result of equal diagnostic quality and superior results of non-contrast MRA in the aortic root [10, 14, 15]. Moreover, renouncement of gadolinium contrast avoids the risk of nephrogenic systemic fibrosis, allergic reactions and contrast material paravasation [16]. However, previous studies are limited by small study populations with different aortic pathologies [17]. Bannas et al. compared contrast-enhanced 3D MRA of the thoracic aorta with non-contrast 3D SSFP imaging in patients with suspected MFS [15]. However, 3D SSFP imaging requires respiratory gating and long acquisition times of up to 10 min [15].

The aim of the present study was to assess whether non-contrast 2D SSFP imaging allows for exact and risk-less monitoring of aortic diameters in patients with MFS. We performed an intraindividual comparison of ECG-gated non-contrast 2D SSFP imaging and routinely performed non-ECG-gated contrast-enhanced 3D MRA exclusively in patients with genetically confirmed MFS. Since the indication for preventive replacement of the aortic root depends on the diameter of the sinuses of Valsalva, we used echocardiography at this level as a standard of reference to validate the accuracy of MRI diameter measurements.

## Material and methods

### Study population

Fifty adult patients (24 male, 26 female; age range 18–73 years; mean 34.7±13.8 years; median 31 years) with confirmed MFS and prior to aortic surgery were included in this prospective cohort study and received MRI and echocardiography between January 2012 and March 2013. Patients younger than 18 years, with contraindications concerning MRI or with aortic surgery in the past were excluded. The local University Marfan Center associated with the University Heart Center established each MFS diagnosis on the basis of evaluation according to the latest Ghent nosology as well as genetic analyses with sequencing of the *FBN1* gene [1, 9]. Each patient was diagnosed with a causative *FBN1* mutation. The study was approved by the institutional review board and all patients provided written informed consent.

### MR imaging

MR Imaging was performed using a 1.5-T system equipped with a five-channel coil for cardiac imaging (Philips Achieva 1.5 T, Philips Medical Systems, Best, the Netherlands). ECG leads were placed in a typical manner for cardiac triggering. Scout images in axial, coronal and sagittal orientation were performed at the beginning of every examination.

### ECG-gated non-enhanced 2D steady state free precession imaging

ECG-gated non-contrast 2D SSFP imaging with sensitivity encoding (SENSE) was acquired in para-sagittal orientation aligned with the curvature of the aortic arch. Image acquisition was triggered to the end-diastolic phase of the cardiac cycle for minimization of motion artefacts during end-expiratory breath-hold [9]. Image parameters were as follows: TR/TE, 3.2/1.6 ms; flip angle, 90°; field of view, 430 mm×302 mm; matrix, 256×180; pixel size, 1.7 mm×1.7 mm; slice thickness, 10 mm; SENSE factor, 2. Number of slices, 20; acquisition time 18–22 s depending on the patient's heart rate.

### Non-ECG-gated contrast-enhanced 3D MRA

Non-ECG-gated contrast-enhanced 3D MRA (CE-MRA) of the entire thoracic aorta was performed after automatic injection (2 ml/s) of gadopentetate dimeglumine (Gd-DTPA, Magnevist, Bayer-Schering Pharma AG, Berlin, Germany) at a dose of 0.2 mmol/kg body weight into an antecubital vein. Scanning parameters of the para-sagittal gradient-echo T1-weighted sequence were TR/TE, 4.8/1.4 ms; flip angle, 40°; field of view, 450×360×90–130 mm; matrix, 368×189×25–36. True spatial resolution was 1.2×1.9×3.6 $mm^3$, interpolated to 0.9×0.7×3.6 mm (512×512 matrix). The time of arrival of contrast in the thoracic aorta was determined with a 2-ml test bolus to calculate the scan delay and to optimize contrast bolus timing. The 3D MRA was performed during a single end-expiration breath-hold. Imaging time varied depending on patient anatomy and field of view (18–24 s).

### MR image evaluation

Anonymised images of non-ECG-gated 3D CE-MRA and ECG-gated non-contrast 2D SSFP images were presented to two radiologists, S.V. and P.B., in random order. The external aortic diameter was measured perpendicular to the blood-filled lumen [9]. Measurements were performed on the identically orientated para-sagittal source images of the non-ECG-gated 3D CE-MRA and of the ECG-gated non-contrast 2D SSFP. Readers were free to choose appropriate slices displaying the maximal profile of the aorta from the stacks of para-sagittal images. No secondary multiplanar reformations (MPR) were used for the comparison of the two techniques. Using the identically oriented para-sagittal images avoided user influence introduced by individually performed MPRs and allowed for assessment of only the differences that are attributed to the different imaging and triggering techniques [15]. Measuring points were determined in the aortic bulbus at the sinuses of Valsalva, the sinotubular junction, the ascending and descending aorta each on the level of the pulmonary trunk and the mid aortic arch between the branching of the left carotid and the left subclavian artery (Fig. 1) [9, 18]. Diameters were measured three times in each image series: For assessment of intraobserver agreement, two measurements were performed by S.V., with an interval of 4 weeks between the first and second measurement. For assessment of interobserver agreement, a third measurement was performed by P.B. Image quality was assessed in consensus by both observers on a three-point scale regarding sharpness, anatomic delineation and presence of motion artefacts at the levels of measurement: 3, excellent image quality; 2, moderate image quality; 1, poor image quality.

### Echocardiography

Out of the 50 patients who received MRI, 48 patients underwent a routine 2D transthoracic echocardiographic examination on the same day and formed a reference group. Aortic diameters at the level of sinuses of Valsalva measured by echocardiography were used to evaluate the accuracy of the diameters obtained from 2D SSFP and 3D CE-MRA. Echocardiography was performed either by M.R. (11 years of experience) or by S.S. (7 years of experience) at the University Heart Center with a commercially available ultrasound system (Sonos 2000, Hewlett Packard, Andover, MA, USA). End-diastolic aortic root diameters were determined using the leading edge method in the parasternal long axis view at the level of the sinuses of Valsalva [19].

### Statistical analysis

Intraclass correlation coefficient (ICC) was calculated to investigate intraobserver and interobserver agreement between measurements obtained from non-ECG-gated 3D CE-MRA and ECG-gated non-contrast 2D SSFP data sets. Bland–Altman analysis was used to assess intra- and interobserver agreement between measurements obtained from 3D CE-MRA and 2D SSFP. A two-sided *t* test was performed for comparison of mean differences and *F* test for comparison of variances. Comparisons of image quality of the aortic root using 3D CE-MRA and 2D SSFP were performed using the Wilcoxon matched-pair test.

Pearson's correlation was calculated to determine the correlation between diameters assessed by non-ECG-gated 3D CE-MRA, ECG-gated non-contrast 2D SSFP and echocardiography. Correlation coefficients greater than 0.8 indicated strong correlation, 0.5–0.8 indicated moderate correlation, 0.3–0.49 indicated weak correlation and coefficients smaller than 0.3 were interpreted as nonexistent correlation. Bland–Altman analysis was used to assess agreement between measurements obtained from 3D CE-MRA 2D SSFP data sets. A two-sided paired *t* test was used to determine significance of differences between measurements obtained from 3D CE-MRA, 2D SSFP and echocardiography. Bland–Altman analyses were also used to assess the agreement between diameters acquired by echocardiography and by 3D CE-MRA and 2D SSFP, respectively.

*P* values less than 0.05 were considered as significant. Statistical analysis was performed using SPSS vers. 20.0 (IBM, Armonk, NY, USA) and Excel (Microsoft Corporation, Redmond, WA, USA). Graphs were created using Prism vers. 5.0 (GraphPad Software Inc., La Jolla, CA, USA).

## Results

All patients were in sinus rhythm and all MR imaging studies were performed without any complication. All studies had

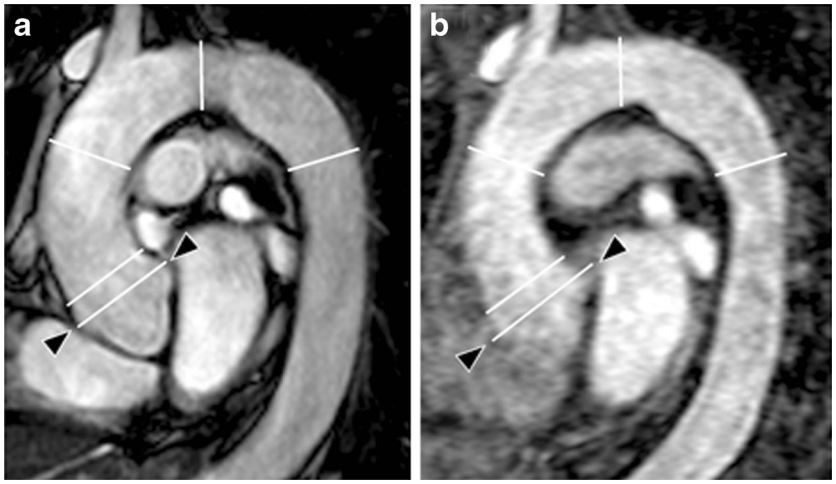


**Fig. 1** **a** Para-sagittal ECG-gated non-contrast 2D SSFP and **b** non-ECG-gated contrast-enhanced 3D MRA of a 60-year-old female patient with confirmed Marfan syndrome. *White lines* indicate the measurement points of the thoracic aorta. From *proximal* to *distal*: Sinuses of Valsalva, sinotubular junction, ascending aorta, aortic arch and descending aorta. Compared to the non-ECG-gated contrast-enhanced 3D MRA with a blurred appearance of the aortic root (**b**, *arrowheads*), the ECG-gated non-contrast 2D SSFP sequence provides a better delineation of the aortic root with a better differentiation of the blood-filled lumen from the aortic wall structures (**a**, *arrowheads*). Both readers rated the image quality at the level of the sinuses of Valsalva as 3 points for SSFP and as 2 points for CE-MRA. Therefore the non-contrast 2D SSFP sequence allows for a more precise measurement at the aortic root owing to the absence of motion artefacts

diagnostic image quality. None of the patients had an aortic dissection and no study was excluded from the evaluation.

## Intraobserver agreement

Intraobserver correlation showed good results with $r>0.8$ for both techniques at all points of measurements (Table 1). Intraobserver correlation concerning the aortic root (sinuses of Valsalva and sinotubular junction) was higher in ECG-gated non-contrast 2D SSFP than in non-ECG-gated 3D CE-MRA. The highest intraobserver agreement was found for the sinuses of Valsalva in 2D SSFP images with $r=0.962$ as compared to 3D CE-MRA with $r=0.864$.

Bland–Altman analyses revealed a smaller intraobserver bias for the ECG-gated non-contrast 2D SSFP at the sinuses of Valsalva (mean difference, 0.01 mm) compared to non-

**Table 1** Intraobserver variance of the measured aortic diameters as determined by non-ECG-gated contrast-enhanced 3D MRA (CE-MRA) and ECG-gated non-contrast 2D SSFP as described by Bland and Altman

| | Intraobserver variance | | | | |
|---|---|---|---|---|---|
| | Sinuses of Valsalva | Sinotubular Junction | Ascending aorta | Mid aortic arch | Descending aorta |
| | Non-ECG-gated CE-MRA | | | | |
| Mean difference (mm) | 0.46 | 0.72 | 0.30 | −0.02 | −0.20 |
| Limits of agreement (mm) | −6.4 to 7.3 | −5.7 to 7.2 | −3.2 to 3.8 | −3.2 to 3.8 | −3.2 to 2.8 |
| Standard deviation (mm) | 3.5 | 3.3 | 1.8 | 2.0 | 1.5 |
| Variance ($mm^2$) | 12.1 | 10.8 | 3.2 | 3.9 | 2.3 |
| Intraclass correlation coefficient ($r$) | 0.86 | 0.85 | 0.93 | 0.82 | 0.98 |
| | ECG-gated SSFP | | | | |
| Mean difference (mm) | 0.01 | 0.78 | 0.10 | −0.30 | 0.09 |
| Limits of agreement (mm) | −3.1 to 3.1 | −3.7 to 5.3 | −3.8 to 4.0 | −3.5 to 2.9 | −2.8 to 2.8 |
| Standard deviation (mm) | 1.6 | 2.3 | 2.0 | 1.6 | 1.4 |
| Variance ($mm^2$) | 2.5 | 5.3 | 4.0 | 2.7 | 2.1 |
| Intraclass correlation coefficient ($r$) | 0.96 | 0.92 | 0.93 | 0.91 | 0.90 |
| $p$ value ($t$ test) | 0.34 | 0.91 | 0.58 | 0.46 | 0.50 |
| $p$ value ($F$ test) | **0.002** | **0.014** | 0.43 | 0.22 | 0.70 |

ICC values are given for both sequence types. $T$ test was performed for comparison of mean differences and $F$ test for comparison of variances. Significant differences are in bold (significant at $p<0.05$)

ECG-gated 3D CE-MRA (mean difference, 0.46 mm) without statistical significance ($p$=0.34).

Concerning variances of measurements, ECG-gated non-contrast 2D SSFP imaging provided significantly smaller variances at the sinuses of Valsalva (2D SSFP, 95 % limits of agreement ±3.1 mm vs. 3D CE-MRA, ±6.9 mm; $p$=0.002) and at the sinotubular junction (2D SSFP, 95 % limits of agreement ±4.5 mm vs. 3D CE-MRA, ±6.5 mm; $p$=0.014). Detailed results of the measurements are given in Table 1. Figure 2a, b illustrate results of Bland–Altman analysis of non-ECG-gated 3D CE-MRA and ECG-gated non-contrast 2D SSFP imaging for intraobserver agreement at the sinuses of Valsalva.

## Interobserver agreement

Analysis of the interobserver correlation showed good results with $r$>0.85 for both techniques at all points of measurements (Table 2). The interobserver agreement was higher in non-contrast 2D SSFP imaging than in contrast-enhanced 3D MRA at all points but the descending aorta where the ICC showed comparable results. Highest interobserver agreement was found for the sinuses of Valsalva in non-contrast 2D SSFP images with $r$=0.974 as compared to contrast-enhanced 3D MRA with $r$=0.908.

Bland–Altman analyses revealed a smaller interobserver bias for the non-contrast 2D SSFP at the sinuses of Valsalva and at the sinotubular junction (mean difference, −0.38 mm and −0.36 mm, respectively) compared to contrast-enhanced 3D MRA (mean difference, −0.72 mm and 0.86 mm, respectively), without statistical significance ($p$=0.53 and $p$=0.06, respectively). Detailed results of measurements are given in Table 2.

Non-contrast 2D SSFP imaging provided significantly smaller variances at the sinuses of Valsalva (2D SSFP, 95 % limits of agreement, ±3.7 mm vs. 3D CE-MRA, ±5.9 mm; $p$=0.002), at the sinotubular junction (2D SSFP, 95 % limits of agreement, ±5.5 mm vs. 3D CE-MRA, ±7.3 mm; $p$=0.043), at the ascending aorta (2D SSFP, 95 % limits of agreement, ±3.0 mm vs. 3D CE-MRA, ±4.8 mm; $p$=0.001) and at the aortic arch (2D SSFP, 95 % limits of agreement, ±2.7 mm vs. 3D CE-MRA, ±4.1 mm; $p$=0.004). Detailed results of measurements are given in Table 2. Figure 2c and d illustrate results of Bland–Altman analysis of contrast-enhanced 3D MRA and non-contrast 2D SSFP imaging for interobserver agreement at the sinuses of Valsalva.

## Comparison of contrast-enhanced 3D MRA and non-contrast 2D SSFP imaging

Pearson's correlation analyses revealed strong correlation of diameters obtained by contrast-enhanced 3D MRA and non-contrast 2D SSFP imaging at all levels ($r$>0.8) (Table 3). Of note, significantly higher diameters were observed when using

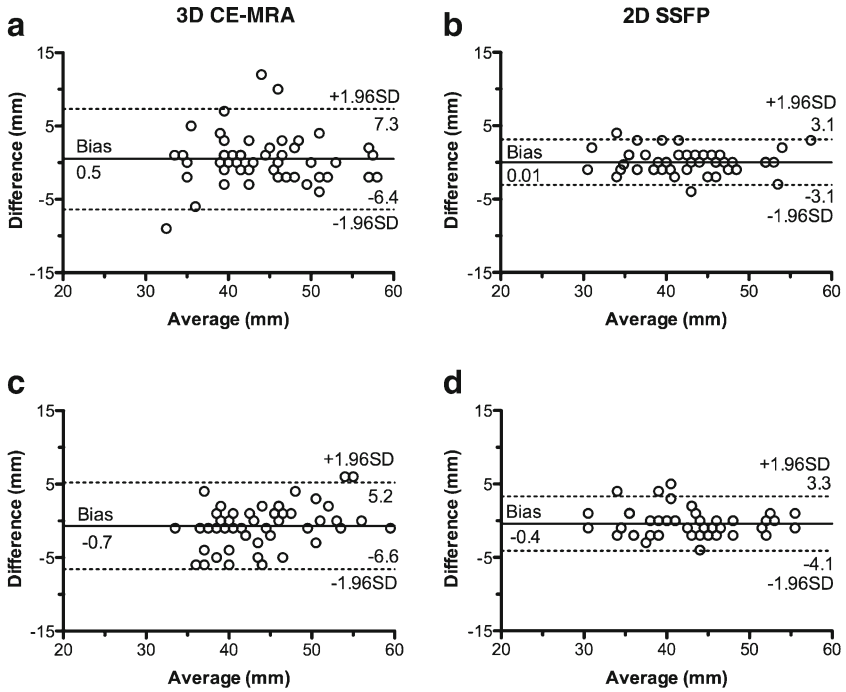


**Fig. 2** Intra- and interobserver agreement of diameter measurements at the sinuses of Valsalva. Bland–Altman plots of the intraobserver agreement for contrast-enhanced 3D MRA (**a**) and non-contrast 2D SSFP (**b**) illustrate the significantly higher intraobserver variance of the non-ECG-gated contrast-enhanced MRA compared to the ECG-gated SSFP sequence ($p$=0.002). Bland–Altman plots of the interobserver agreement for contrast-enhanced 3D MRA (**c**) and non-contrast 2D SSFP (**d**) illustrate the higher interobserver variance of the non-ECG-gated contrast-enhanced 3D MRA compared to the ECG-gated SSFP sequence ($p$=0.002). *Middle solid line* indicates the mean bias of the diameter measurements, the *dotted lines* indicate the 95 % confidence interval

**Table 2** Interobserver variance of the measured aortic diameters as determined by non-ECG-gated contrast-enhanced 3D MRA (CE-MRA) and ECG-gated non-contrast 2D SSFP as described by Bland and Altman

| | Interobserver variance | | | | |
|---|---|---|---|---|---|
| | Sinuses of Valsalva | Sinotubular junction | Ascending aorta | Mid aortic arch | Descending aorta |
| | Non-ECG-gated CE-MRA | | | | |
| Mean difference (mm) | −0.72 | 0.86 | 0.15 | 1.22 | −0.14 |
| Limits of agreement (mm) | −6.6 to 5.1 | −6.5 to 8.2 | −4.6 to 4.9 | −2.9 to 5.4 | −2.6 to 2.4 |
| Standard deviation (mm) | 3.0 | 3.8 | 2.4 | 2.1 | 1.3 |
| Variance ($mm^2$) | 9.0 | 14.2 | 5.9 | 4.5 | 1.6 |
| Intraclass correlation coefficient ($r$) | 0.91 | 0.86 | 0.93 | 0.89 | 0.96 |
| | ECG-gated SSFP | | | | |
| Mean difference (mm) | −0.38 | −0.36 | 0.36 | 1.02 | 0.34 |
| Limits of agreement (mm) | −4.1 to 3.3 | −5.9 to 5.2 | −2.6 to 3.3 | −1.7 to 3.7 | −2.4 to 3.1 |
| Standard deviation (mm) | 1.9 | 2.8 | 1.5 | 1.4 | 1.4 |
| Variance ($mm^2$) | 3.6 | 7.9 | 2.3 | 1.9 | 20.0 |
| Intraclass correlation coefficient ($r$) | 0.97 | 0.94 | 0.97 | 0.96 | 0.96 |
| $p$ value ($t$ test) | 0.53 | 0.06 | 0.58 | 0.53 | 0.11 |
| $p$ value ($F$ test) | **0.002** | **0.043** | **0.001** | **0.004** | 0.50 |

ICC values are given for both sequence types. $T$ test was performed for comparison of mean differences and $F$ test for comparison of variances. Significant differences are in bold (significant at $p<0.05$)

non-ECG-gated 3D CE-MRA compared to ECG-gated non-contrast 2D SSFP imaging at the sinuses of Valsalva (mean bias, 2.5 mm; $p<0.0001$) (Fig. 3) and descending aorta (mean bias, 0.8 mm; $p=0.0001$) (Table 3). The mean absolute diameter at the sinuses of Valsalva was 42±6 mm when using 2D SSFP and 44±5 mm when using contrast-enhanced 3D MRA. Detailed results of measurements are given in Table 3, upper rows.

## Image quality of contrast-enhanced 3D MRA and non-contrast 2D SSFP imaging

2D SSFP imaging yielded significantly better image quality scores than contrast-enhanced 3D MRA at the sinus of Valsalva ($p<0.0001$), sinotubular junction ($p<0.0001$) and the ascending aorta ($p=0.02$). Image quality of the aortic arch ($p=0.42$) and descending aorta ($p=0.64$) showed no significant differences between both techniques. Detailed results of image quality ratings are given in Table 4. ECG-gated non-contrast 2D SSFP allowed superior depiction of the aortic root with sharper delineation of the blood-filled lumen from the wall structures than non-ECG-gated contrast-enhanced 3D MRA (Fig. 1).

## Comparison of aortic root diameter measurements in MRI and echocardiography

Pearson's correlation analyses revealed strong correlations between both MRA techniques and echocardiographic diameter measurements at the sinuses of Valsalva, however

**Table 3** Comparison of aortic diameters as determined by contrast-enhanced 3D MRA (CE-MRA) and non-contrast 2D SSFP as described by Bland and Altman

| SSFP vs. CE-MRA | Sinuses of Valsalva | Sinotubular junction | Ascending aorta | Aortic arch | Descending aorta |
|---|---|---|---|---|---|
| Mean diameter SSFP (mm) | 42.1±6.2 | 31.6±5.4 | 30.0±5.2 | 24.2±3.4 | 24.1±3.4 |
| Mean diameter CE-MRA (mm) | 44.4±5.4 | 32.1±4.9 | 30.4±4.9 | 24.6±3.4 | 24.7±3.1 |
| Mean difference (mm) | −2.5 | −0.5 | −0.4 | −0.2 | −0.8 |
| Limits of agreement (mm) | −7.8 to 2.9 | −6.9 to 5.9 | −1.1 to 0.2 | −3.3 to 2.9 | −3.5 to 1.9 |
| Standard deviation (mm) | 2.7 | 3.3 | 2.2 | 1.6 | 1.4 |
| Variance ($mm^2$) | 7.3 | 10.9 | 4.9 | 2.6 | 2.0 |
| $p$ value ($t$ test) | <**0.0001** | 0.27 | 0.18 | 0.42 | <**0.001** |
| Pearson's correlation ($r$) | 0.90 | 0.80 | 0.91 | 0.90 | 0.91 |

Pearson's correlation coefficient ($r$) between the different imaging modalities is given. $T$ test was performed for comparison of mean differences. Significant differences are in bold (significant at $p<0.05$)

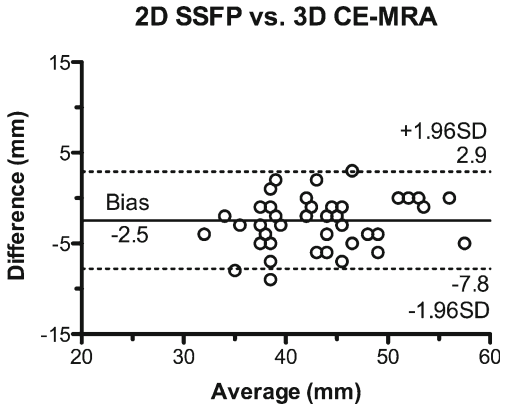


**Fig. 3** Bland–Altman comparison of the measured diameters at the sinuses of Valsava assessed by contrast-enhanced 3D MRA and non-contrast 2D SSFP. The plot indicates a significant mean difference of −2.5 ±2.9 mm for 2D SSFP compared to 3D CE-MRA ($p<0.0001$). *Middle solid line* indicates the mean bias of the diameter measurements, the *dotted lines* indicate the 95 % confidence interval

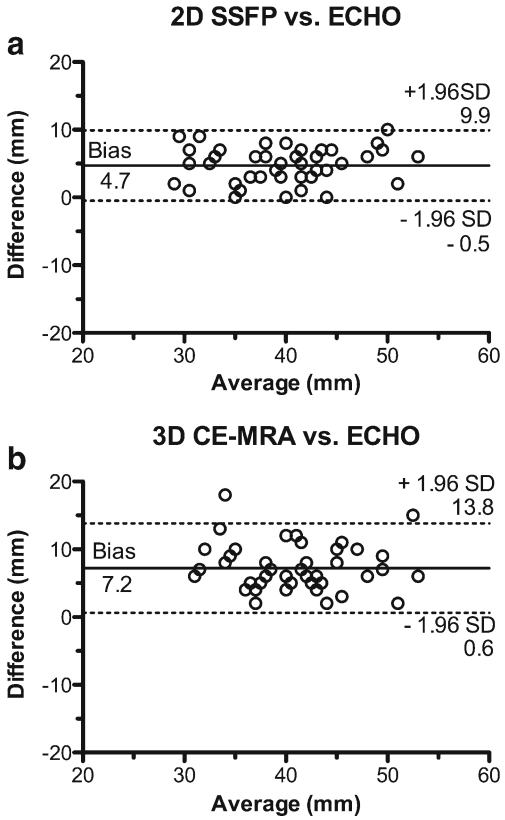


**Fig. 4** Bland–Altman comparison of the measured diameters at the sinuses of Valsava assessed by the two MRA techniques and echocardiography. *Middle solid line* indicates the mean bias of the diameter measurements. The *dotted lines* indicate the 95 % confidence interval. **a** The plot indicates a significant mean difference of 4.7±2.6 mm for 2D SSFP compared to echocardiography ($p<0.0001$). **b** The plot indicates a significant mean difference of 7.2±3.4 mm for 3D CE-MRA compared to echocardiography ($p<0.0001$)

somewhat stronger for the 2D SSFP ($r=0.91$; $p<0.0001$) when compared to 3D CE-MRA with ($r=0.83$; $p<0.0001$). Of note, 2D SSFP and 3D CE-MRA revealed significantly higher diameters (42±6 mm, $p<0.0001$ and 44±5 mm, $p<0.0001$, respectively) as compared to diameters obtained by echocardiography with 37±6 mm. Bland–Altman analysis confirmed a higher bias of 3D CE-MRA (mean difference, 7.2 ±3.4 mm, 95 % limits of agreement, 0.6–13.8 mm) than 2D SSFP (mean difference, 4.7±2.6 mm, 95 % limits of agreement, −0.5 to 9.9 mm) when compared to echocardiographic diameter measurements at the sinuses of Valsalva (Fig. 4).

## Impact on patient management

The observed bias of −2.5 mm between 2D SSFP imaging and contrast-enhanced 3D MRA led inherently to differences between both imaging techniques in identification of patients with a diameter of the sinuses of Valsalva greater than 45 mm, which is used in our university expert centre as the threshold diameter for aortic root replacement (Fig. 5) [8]. In 12 patients contrast-enhanced 3D CE-MRA revealed a diameter greater than 45 mm, which could be confirmed by non-contrast 2D SSFP imaging in 10 patients. Six of the 10 patients that were correctly identified with both imaging techniques successfully underwent subsequent aortic root replacement. The remaining patients refused prophylactic aortic root surgery and underwent close follow-up monitoring. The two patients with borderline diameters and no further risk factors and the two patients with sinuses of Valsalva greater than 45 mm that were only identified by CE-MRA underwent close follow-up monitoring as well. The differences of the determined diameters were 1 mm (2D SSFP, 44 mm vs. 3D CE-MRA, 45 mm) and 3 mm (2D SSFP, 43 mm vs. 3D CE-MRA, 46 mm).

**Table 4** Mean subjective image scores at the 5 points of measurement defined by consensus reading for contrast-enhanced 3D MRA (CE-MRA) and non-contrast 2D SSFP

| | Sinuses of Valsalva | Sinotubular junction | Ascending aorta | Aortic arch | Descending aorta |
|---|---|---|---|---|---|
| SSFP | 2.5 | 2.6 | 2.6 | 2.7 | 2.7 |
| CE-MRA | 1.5 | 1.6 | 2.3 | 2.6 | 2.7 |
| *p* value (Wilcoxon matched-pair) | **<0.0001** | **<0.0001** | **0.02** | 0.42 | 0.64 |

A three-point scale was used: 3, excellent image quality; 2, moderate image quality; 1, poor image quality. Wilcoxon matched-pair analysis was used for comparison of differences. Significant differences are in bold (significant at $p<0.05$)

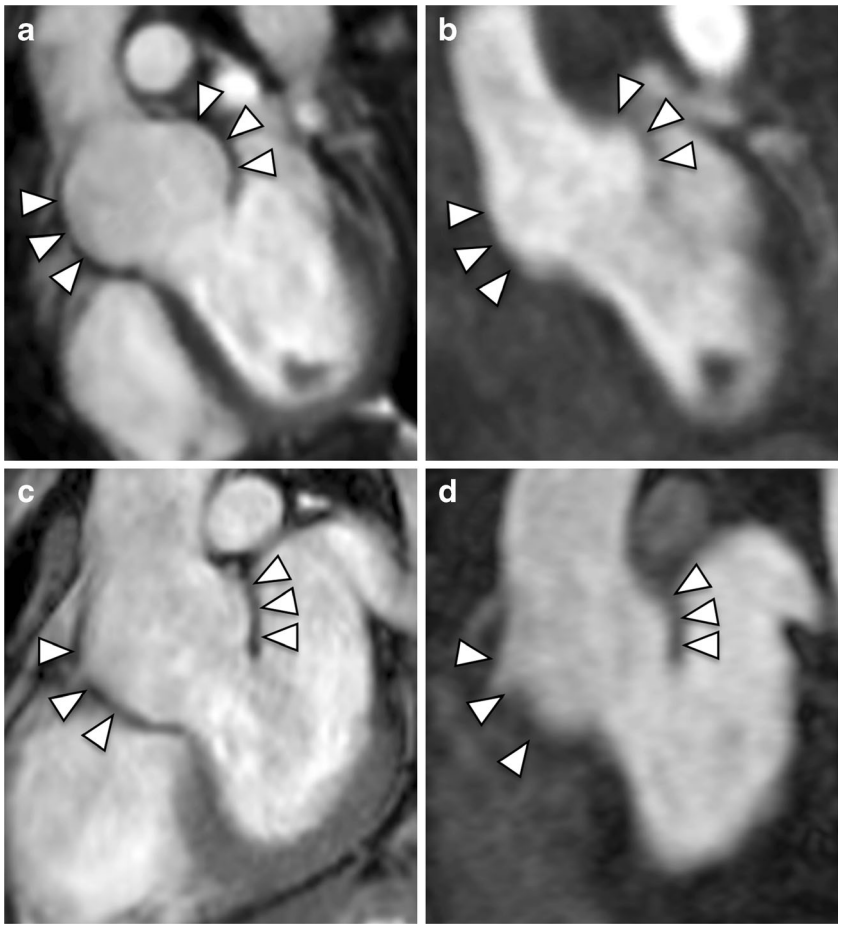


**Fig. 5** **a**, **c** Non-contrast 2D SSFP and **b**, **d** contrast-enhanced 3D MRA in **a**, **b** a 29-year-old man and **c**, **d** a 39-year-old man both with confirmed MFS. A diameter of the sinuses of Valsalva of greater than 50 mm was detected in both sequences (SSFP, 52 mm; CE-MRA 53 mm and SSFP, 54 mm; CE-MRA 53 mm, respectively). As result of the MRA examination both patients were referred to preventive surgery and successfully underwent aortic root replacement pursuant to David's procedure. Note the clear delineation of the aortic root when using the ECG-gated non-contrast 2D SSFP sequence (**a**, **c**, *arrowheads*) as compared to the blurred appearance of the aortic root when using non-ECG-gated contrast-enhanced 3D MRA (**b**, **d**, *arrowheads*). Both readers rated the image quality at the level of the sinuses of Valsalva as 3 points for SSFP and as 2 points for CE-MRA in both patients

## Discussion

We prospectively compared diameter measurements of the thoracic aorta in non-ECG-gated contrast-enhanced 3D MRA and ECG-gated non-contrast 2D SSFP imaging in 50 adult patients with confirmed MFS and prior to aortic surgery. The indication for preventive replacement of the aortic root depends on the diameter of the sinuses of Valsalva. Hence, the focus of our study was the comparison of the precision and quality of the aortic measurements at this locus in contrast-enhanced 3D MRA and non-contrast 2D SSFP imaging using echocardiography as reference standard. Non-contrast 2D SSFP imaging revealed higher intra- and interobserver agreement and intraclass correlations than contrast-enhanced 3D MRA concerning measurements of aortic root diameters. Consistently, the subjective image quality was markedly better for non-contrast 2D SSFP, especially at the aortic root. Intraindividual comparison revealed significant higher diameters of the sinuses of Valsalva when using contrast-enhanced 3D MRA compared to non-contrast SSFP imaging, which could be confirmed by echocardiography.

Improved image quality of ECG-gated non-contrast 2D SSFP imaging compared to non-ECG-gated contrast-enhanced 3D MRA of the thoracic aorta in unselected patient populations has been stated by several studies [20, 21]. Interestingly, the superior image quality of non-contrast ECG-gated SSFP imaging has also been demonstrated when compared with state-of-the-art ECG-gated CE-MRA [10]. Bannas et al. compared ECG-triggered non-contrast 3D SSFP imaging with a non-ECG-triggered contrast-enhanced 3D MRA in 51 patients with a suspected syndromic presentation of ascending aortic aneurysm of whom 38 were subsequently diagnosed with MFS [9, 15]. Their investigations confirmed improved image quality of ECG-gated non-contrast 3D SSFP imaging and additionally revealed higher reliability and reproducibility of aortic root measurements. However, 3D SSFP imaging requires respiratory gating and long acquisition times of up to 10 min [15, 22].

The rapid 2D SSFP sequence tested in this study provided significantly better image quality of the aortic root and the ascending aorta as compared to contrast-enhanced 3D MRA. The aortic arch and the descending aorta showed no significant differences. As the proximal parts of the aorta move constantly during the cardiac cycle, this observation can be assigned to the decreased motion artefacts resulting from ECG-triggering and imaging in the end-diastolic phase [11, 12, 15] which leads to a sharper delineation of the aortic wall and its excellent delimitation from the blood-filled lumen. In

contrast, non-ECG-gated contrast-enhanced 3D MRA tends to blend the aortic wall structures and the contrast-filled lumen merge into one another at the level of the aortic root as a result of continuous acquisition during the cardiac cycle. Accordingly, significantly better reproducibility of the aortic root diameters (greater intra- and interobserver agreement) can be explained by the decrease of motion artefacts with this ECG-gated technique.

Moreover, significant larger diameters were determined with non-ECG-gated contrast-enhanced 3D MRA at the sinuses of Valsalva as compared to ECG-gated non-contrast SSFP imaging. This may also be explained by the acquisition of the non-ECG-gated contrast-enhanced 3D MRA throughout the cardiac cycle, which gives rise to an image (and subsequently to the measured diameters) comprising information from systole and diastole, during which the aortic diameter changes physiologically. Hence, assessing the aortic diameters with this imaging technique is not only imprecise because of image blurring, but also overestimates the diameter compared to measurements which are acquired during diastole, as recommended by the guidelines [9]. In contrast, ECG-gated SSFP imaging triggered to the end-diastolic phase of the cardiac cycle allows exact delimitation and measurements of the aortic wall during diastole (Fig. 4). Recent studies have shown that ECG-gating also improves the image quality of contrast-enhanced MRA [23]. However, since we aimed to avoid the use of contrast material in patients with MFS we do not pursue these ECG-gated contrast-enhanced techniques at our institution.

Beside other factors like aneurysm morphology, the indication for preventive aortic root replacement depends on absolute aortic root diameters at the sinuses of Valsalva and the rate of enlargement. Actual guidelines recommend preventive surgery at a threshold diameter of 5.0 cm but expert centres with very good surgical outcome perform surgery at 4.5 cm because 15 % of MFS patients present with aortic dissection at diameters of 5.0 cm or less [5, 24]. In our study 10 patients presented with aortic root diameters greater than 4.5 cm and were correctly identified with both imaging techniques. Six of them successfully underwent subsequent prophylactic aortic root replacement. Non-ECG-gated contrast-enhanced 3D CE-MRA yielded two more patients with diameter measurements greater than 4.5 cm, which could not be confirmed by the ECG-gated SSFP technique or echocardiography. The differences of the determined diameters in these patients between the two MRA techniques are explained by the overall observed difference of −2.5 mm for measurements at the sinuses of Valsalva.

Annual MRA is recommended for ideal monitoring of the aortic root dimension. Accordingly, MFS patients have to undergo a considerable number of MRI exams during their life. Although contrast-enhanced MRA has been shown to be suitable for aortic monitoring, it bears the risk of evoking nephrogenic systemic fibrosis or causing paravasation [16, 25, 26]. In this context, the renunciation of gadolinium contrast agents implies the avoidance of the mentioned adverse effects or complications. Moreover, non-contrast enhanced MRA facilitates the clinical routine and allows for an acceleration of the imaging process. With an acquisition time of less than 1 min, compared to the 3D SSFP introduced by Bannas et al. with 8.3±2.4 min and contrast-enhanced 3D MRA with greater than 10 min (placing and connection of the intravenous line, test bolus, pre- and post-contrast imaging, image post processing), the use of the applied non-contrast 2D SSFP sequence provides an additional advantage for clinical routine application [15, 17].

This study revealed an average bias of 2.5 mm for aortic diameters measured with non-ECG-gated contrast-enhanced vs. ECG-gated non-contrast MRA at the sinuses of Valsalva. Furthermore, a significant offset has to be taken into consideration when comparing diameters of the sinuses of Valsalva of para-sagittal MRA measurements with results of transthoracic echocardiography owing to different orientations of the performed measurements, reflecting the oval shape of the aortic root, as stated by recent studies [27, 28]. Moreover, we performed echocardiographic measurements of the ascending aorta in the leading edge technique as recommended by current guidelines [19]. This means that diameters are taken from the outer margin of the aortic wall, which is located close to the ultrasound transducer, to the inner margin of the distant wall [29]. In contrast, current guidelines recommend measuring the external aortic diameters in MRA [9]. Hence, the different measurement techniques inherently lead to a bias based on the average aortic wall thickness of ca. 2.4 mm [30]. In conclusion, ca. 2.4 mm of the observed total bias between echocardiography and MRA in this study (3D CE-MRA, 7.2± 3.4 mm; 2D SSFP, 4.7±2.6 mm) can be ascribed to different measurement techniques (leading edge vs. outer wall to outer wall). In summary, we recommend maintaining the same single imaging technique for longitudinal follow-up of aortic diameters and assessment of expansion rates over time. Concerning MRA, using ECG-gated non-contrast 2D SSFP imaging for monitoring of the thoracic aorta is favourable, because of higher observer agreement, better image quality, improved delineation of the aortic root and acceleration of the imaging process. In consequence of this study, we stopped application of intravenous gadolinium contrast material for preoperative assessment of thoracic aorta in patients with MFS at our institution and did not encounter any disadvantages. As another consequence we added cardiac cine MRI of the aortic root in LVOT view and three-chamber view to the clinical protocol. Particularly in cases were aortic diameters approach the threshold, these sequences are useful to allow sharp evaluation throughout the cardiac cycle.

It may be regarded as a limitation that the diameters were only determined in the para-sagittal planes (along the flow

axis of the aorta) of the source images and no secondary MPRs were performed. Studies have shown that the measured diameter depends on the orientation of the images owing to the oval configuration of the aorta [15, 27]. As the orientations of both compared sequences were identical, we believe that a secondary reformation would not have provided different results in terms of the technique comparison. However, in clinical practice, particularly when the aortic diameter reaches the critical threshold, secondary MPRs or dedicated cardiac cine MRI of the aortic root should be performed to assess the maximal diameter of the aortic root in different orientations.

## Conclusion

ECG-gated non-contrast 2D SSFP imaging is an appropriate alternative for initial assessment and monitoring of the aortic root in patients with Marfan syndrome. Our study revealed that ECG-gated non-contrast SSFP imaging provides superior image quality with sharper delimitation of the aortic root resulting in better reproducibility and higher accuracy of the diameter measurements compared to non-ECG-gated contrast-enhanced 3D imaging. Moreover, renouncement of intravenous gadolinium contrast avoids its associated adverse effects and complications.

**Acknowledgements** The scientific guarantor of this publication is Dr. Peter Bannas. The authors of this manuscript declare no relationships with any companies whose products or services may be related to the subject matter of the article. The authors state that this work has not received any funding. One of the authors has significant statistical expertise. Institutional review board approval was obtained. Written informed consent was obtained from all subjects (patients) in this study. No study subjects or cohorts have been previously reported. Methodology: prospective, diagnostic or prognostic study, performed at one institution.

## References

1. Loeys BL, Dietz HC, Braverman AC et al (2010) The revised Ghent nosology for the Marfan syndrome. J Med Genet 47:476–485
2. Murdoch JL, Walker BA, Halpern BL et al (1972) Life expectancy and causes of death in the Marfan syndrome. N Engl J Med 286:804–808
3. Silverman DI, Burton KJ, Gray J et al (1995) Life expectancy in the Marfan syndrome. Am J Cardiol 75:157–160
4. von Kodolitsch Y, Rybczynski M, Detter C, Robinson PN (2008) Diagnosis and management of Marfan syndrome. Futur Cardiol 4: 85–96
5. Gott VL, Greene PS, Alejo DE et al (1999) Replacement of the aortic root in patients with Marfan's syndrome. N Engl J Med 340: 1307–1313
6. Bernhardt AMJ, Treede H, Rybczynski M et al (2011) Comparison of aortic root replacement in patients with Marfan syndrome. Eur J Cardiothorac Surg 40:1052–1057
7. Hiratzka LF, Bakris GL, Beckman JA et al (2010) 2010 ACCF/AHA/AATS/ACR/ASA/SCA/SCAI/SIR/STS/SVM guidelines for the diagnosis and management of patients with thoracic aortic disease. JAC 55:e27–e129
8. von Kodolitsch Y, Robinson PN, Berger J (2014) When should surgery be performed in Marfan syndrome and other connective tissue disorders to protect against type A dissection? In: Bonser RS, Pagano D, Haverich A, Mascaro J (eds) Controversies in aortic dissection and aneurysmal disease. Springer, New York, p 17
9. Hiratzka LF, Bakris GL, Beckman JA et al (2010) 2010 ACCF/AHA/AATS/ACR/ASA/SCA/SCAI/SIR/STS/SVM guidelines for the diagnosis and management of patients with thoracic aortic disease. A report of the American College of Cardiology Foundation/American Heart Association Task Force on Practice Guidelines, American Association for Thoracic Surgery, American College of Radiology, American Stroke Association, Society of Cardiovascular Anesthesiologists, Society for Cardiovascular Angiography and Interventions, Society of Interventional Radiology, Society of Thoracic Surgeons, and Society for Vascular Medicine. J Am Coll Cardiol 55:e27–e129
10. von Knobelsdorff-Brenkenhoff F, Gruettner H, Trauzeddel RF et al (2014) Comparison of native high-resolution 3D and contrast-enhanced MR angiography for assessing the thoracic aorta. Eur Heart J Cardiovasc Imaging 15:651–658
11. Russo V, Renzulli M, La Palombara C, Fattori R (2006) Congenital diseases of the thoracic aorta. Role of MRI and MRA. Eur Radiol 16: 676–684
12. François CJ, Hartung MP, Reeder SB et al (2013) MRI for acute chest pain: current state of the art. J Magn Reson Imaging 37:1290–1300
13. Carr JC, Simonetti O, Bundy J et al (2001) Cine MR angiography of the heart with segmented true fast imaging with steady-state precession. Radiology 219:828–834
14. Gebker R, Gomaa O, Schnackenburg B et al (2007) Comparison of different MRI techniques for the assessment of thoracic aortic pathology: 3D contrast enhanced MR angiography, turbo spin echo and balanced steady state free precession. Int J Cardiovasc Imaging 23:747–756
15. Bannas P, Groth M, Rybczynski M et al (2013) Assessment of aortic root dimensions in patients with suspected Marfan syndrome: intraindividual comparison of contrast-enhanced and non-contrast magnetic resonance angiography with echocardiography. Int J Cardiol 167:190–196
16. Wertman R, Altun E, Martin DR et al (2008) Risk of nephrogenic systemic fibrosis: evaluation of gadolinium chelate contrast agents at four American universities. Radiology 248:799–806
17. Groth M, Henes FO, Müllerleile K et al (2012) Accuracy of thoracic aortic measurements assessed by contrast enhanced and unenhanced magnetic resonance imaging. Eur J Radiol 81:762–766
18. Pearson GD, Devereux R, Loeys B et al (2008) Report of the National Heart, Lung, and Blood Institute and National Marfan Foundation Working Group on research in Marfan syndrome and related disorders. Circulation 118:785–791
19. Vriz O, Driussi C, Bettio M et al (2013) Aortic root dimensions and stiffness in healthy subjects. Am J Cardiol. doi:10.1016/j.amjcard.2013.05.068
20. Krishnam MS, Tomasian A, Malik S et al (2010) Image quality and diagnostic accuracy of unenhanced SSFP MR angiography compared with conventional contrast-enhanced MR angiography for the assessment of thoracic aortic diseases. Eur Radiol 20:1311–1320
21. Amano Y, Takahama K, Kumita S (2008) Non-contrast-enhanced MR angiography of the thoracic aorta using cardiac and navigator-gated magnetization-prepared three-dimensional steady-state free precession. J Magn Reson Imaging 27:504–509
22. Holloway BJ, Rosewarne D, Jones RG (2011) Imaging of thoracic aortic disease. Br J Radiol 84:S338–S354
23. Groves EM, Bireley W, Dill K et al (2007) Quantitative analysis of ECG-gated high-resolution contrast-enhanced MR angiography of the thoracic aorta. AJR Am J Roentgenol 188:522–528

24. Rimoin DL, Pyeritz RE, Korf B (eds) (2013) Emery & Rimoin's principles and practice of medical genetics. Academic, Oxford
25. Broome DR (2008) Nephrogenic systemic fibrosis associated with gadolinium based contrast agents: a summary of the medical literature reporting. Eur J Radiol 66:230–234
26. Shellock FG, Spinazzi A (2008) MRI safety update 2008: part 1, MRI contrast agents and nephrogenic systemic fibrosis. AJR Am J Roentgenol 191:1129–1139
27. Koos R, Altiok E, Mahnken AH et al (2012) Evaluation of aortic root for definition of prosthesis size by magnetic resonance imaging and cardiac computed tomography: implications for transcatheter aortic valve implantation. Int J Cardiol 158:353–358
28. Messika-Zeitoun D, Serfaty J-M, Brochet E et al (2010) Multimodal assessment of the aortic annulus diameter: implications for transcatheter aortic valve implantation. J Am Coll Cardiol 55:186–194
29. Muraru D, Maffessanti F, Kocabay G et al (2013) Ascending aorta diameters measured by echocardiography using both leading edge-to-leading edge and inner edge-to-inner edge conventions in healthy volunteers. Eur Heart J Cardiovasc Imaging. doi:10.1093/ehjci/jet173
30. Li AE, Kamel I, Rando F et al (2004) Using MRI to assess aortic wall thickness in the multiethnic study of atherosclerosis: distribution by race, sex, and age. AJR Am J Roentgenol 182:593–597